This is a preprint of a paper that appeared in the Proceedings of IEEE International Symposium on Robot and Human Interactive Communication (RO-MAN), 2014, Edinburgh

Implementation, Control and User-Feedback of the Int^{2}Bot for the Investigation of Lower Limb Body Schema Integration*

P. Beckerle[1,5], F. Schültje[2], J. Wojtusch[3,5], O. Christ[4]

***Abstract*— The integration of prostheses or wearable robotics into the body schema of their users is a fundamental requirement for the acceptance and control of such artificial devices. Duration and progress of integration are primarily influenced by visual, tactile, and proprioceptive perception. This paper describes the Int^{2}Bot, a robot for the assessment of lower limb body schema integration during postural motion. The robot is designed to imitate human squatting movements to investigate the integration of artificial limbs into the body schema. The psychological and technical concepts as well as the mechatronic implementation and control are presented along with interface extensions comprising human knee position sensing and tactile user-feedback. The performance of the robot is examined by experiments excluding and including the human-robot interface and a human user. Those without interface show that the robot itself can perform considerably fast squats with $0.8\,\mathrm{Hz}$, which comes up to maximum human capabilities. The computed torque control achieves good tracking results and fuzzy-based friction compensation further reduces position errors by up to 50%. Yet, results considering the vision-based part of the human-robot interface show that the setup is mainly limited due to delays in motion acquisition with the RGB-D sensor.**

I. INTRODUCTION

With the incident of amputation, well-being and quality of life of people with limb loss are affected [1]. The main changing processes after amputation concern body image and body schema of the amputee [1]. While the body image comprises the psychological experience of the own body, the body schema represents its characteristics in a subconscious, neurophysiological and multisensory way [2], [3] and is linked to the sense of having control over the own body. According to [1], the changes are categorized in three phases: After the first experience of being a person with a disability, actual changes of identity, body image and body schema occur before finally a new identity is formed. Integrating a prosthesis to the body schema and developing a positive self appearance are fostered by individual factors but also counteracted by negative emotions in a psychological adjustment process [1], [2], [4], [5]. The time after amputation is an important factor for body schema integration of a prosthesis [2], [4] and functional limitations seem to have major influence on the well-being and quality of life of the users [4], [2], [1]. Eventually, a functional adaptation to the prosthesis is successful, if artificial and intact extremities are equally integrated and represented in the body schema and body image [2]. Feelings of unrealistic body parts are related to deficits in human information processing and can occur as a part of phantom sensations after amputation [6]. A duration of four years required to re-regulate such sensations can be found [2], [5] and disturbances of body schema and image experience are reported [3].

The body schema can experimentally be manipulated in healthy subjects, as the feeling of the ownership of an artificial limb and a measurable proprioceptive re-calibration could be induced by synchronously brushing the hidden real hand and a visible rubber hand [7]. This effect is referred to as Rubber Hand Illusion (RHI) and seems to be caused by a multisensory integration of visual, tactile and proprioceptive information. A systematic review in [8] considers RHI evoked during movement, its maintaining factors and the stability of the illusion. While it has been shown that performing motor tasks can replace haptic feedback in inducing the illusion, this is not proven for the lower limbs in virtual reality environments up to now [9]. Experimental investigations of RHI with prosthetic hand [10], show that a manipulation of the body schema is a promising approach to improve prosthetic intervention. First investigations on transferring the RHI to the lower limbs in terms of a Rubber Foot Illusion show significant changes in survey data while results differ regarding the proprioceptive drift [11], [12].

This paper deals with implementation, control and user-feedback of a robot aiming at investigating Rubber Foot / Leg Illusions (RFI/RLI). The robot might support future design of prostheses or wearable robotics by RFI/RLI insights [13], [14], as such seem to require embodiment in a robot [9]. Section II explains the psychological approach and extends test design the interfaces between robot and human subject. The extensions aim at investigating RHI/RLI itself as well as the impact possible future interface technologies. Section III shows the implementation of the robot hardware, the real-time control system and the extended interfaces. A dynamics model of the robot, the resulting computed torque controls and a fuzzy-based friction compensation are shown in Section IV. Results from simulations and experiments with and without a human participant are given in Section V. With those, the feasibility of the control approach and practical limitations through the vision-based human-robot interface

*This work was funded by Forum for Interdisciplinary Research of Technische Universität Darmstadt.

[1] Institute for Mechatronic Systems in Mechanical Engineering, Technische Universität Darmstadt, Darmstadt, Germany beckerle@ims.tu-darmstadt.de

[2] Institute for Anthropomatics and Robotics, Karlsruhe Institute of Technology, Karlsruhe, Germany, fabian.schueltje@kit.edu

[3] Simulation, Systems Optimization, and Robotics Group, Department of Computer Science, Technische Universität Darmstadt, Darmstadt, Germany wojtusch@sim.tu-darmstadt.de

[4] Institute Humans in Complex Systems, School of Applied Psychology, University of Applied Sciences and Arts Northwestern Switzerland, Olten, Switzerland, oliver.christ@fhnw.ch

[5] *Member, IEEE*

are revealed. Conclusions and an outlook on future works are finally given in Section VI.

II. INT^{2}BOT CONCEPT

In [13] a test design to investigate a Rubber Leg Illusion (RLI) and its maintaining factors during motion is proposed. Following, the psychological test design and the robotic approach are extended leading to the Int^{2}Bot concept. Experiments are approved by TU Darmstadt ethics committee.

A. Psychological Approach

The robotic device aims at examining the RLI during postural movements, as a lack of satisfaction in postural motor functioning irrespective of the prosthesis technology is indicated by the results of [15]. Since appearance showed to be a descriptor for subjective body schema integration and significantly correlated with satisfaction with postural movements [15], those movements might be used for the assessment of body schema integration - e.g., in user-centered prosthetic design. Independent variables to be assessed in individual groups are the influence of synchronous and asynchronous feedback motivated by [16] as well as the distance between participant and robot, since location showed to be a significant predictor of proprioceptive displacement in [17]. Hence, proprioceptive drift is analyzed and the questionnaire from [17] is completed. Further, the movement velocity and posture can be treated as control variables to understand their impact on the illusions. Important control variables are the issue, if the illusion can occur without imitating movements of the robot, the ambient temperature and ambient sounds. Expectations of the participants and questionnaire response are analyzed as well as proprioceptive drift, electrodermal activity [18], [19] and limb temperature [20] to be used as measures for assessment. An overview on possible variables and measures for test design is given in Table I.

B. Robotic Setup

During the experiments, the robot imitates postural movements of one human leg in sagittal plane, while the participant stands close to the robot. At the same time, the imitated leg of the participant is hidden to enable the occurrence of a RLI regarding the robot. The functional concept of the Int^{2}Bot according to [13] and possible extensions is depicted in Figure 1. The mechanical design imitates foot, shank and thigh as well as the knee and ankle joint in appearance and functionality. To control the robot, an RGB-D sensor performs contactless human motion tracking and the desired

TABLE I

POSSIBLE VARIABLES AND MEASURES FOR RHI/RLI TEST DESIGN.

Independent vari.	Control vari.	Measures
(A)synchronism/delay	No subject movement	Questionnaire
Robot distance	Ambient sound	Proprioceptive drift
Movement velocity	Ambient temperature	Electrodermal act.
Posture		Limb temperature
Tactile feedback		
Kinesthetic feedback		

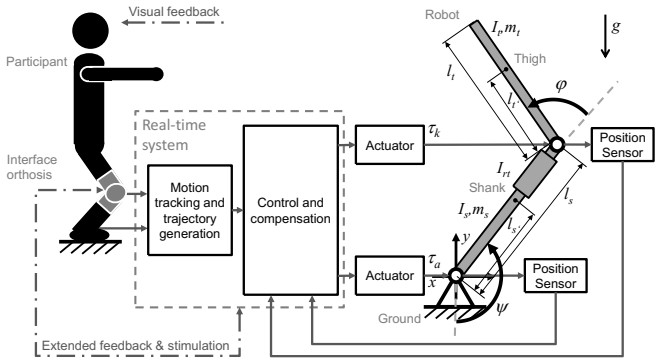

Fig. 1. Functional concept of the Int^{2}Bot: Solid arrows represent signal and power flows. Dash-dotted arrows indicate multi-sensory feedback channels.

robot trajectories are generated from this. This vision-based part of the human-robot interface is extensively dealt with in [21]. Control and compensation algorithms further utilize proprioceptive data from the robot joints.

C. Interface Extensions

To investigate human-robot/prosthesis interface technologies supporting body schema integration in the lower limbs, the user can be equipped with an instrumented and actuated knee orthosis as shown in Figure 1 enabling the examination of additional user-feedback and sensing channels. According to the *Bipolar Man* framework the enlargement of communication flow by using and exploiting more natural/artificial actuators and sensors is required for improving such interfaces [22]. Artificial sensors could be integrated in the knee orthosis and measure human joint positions, electro dermal activity and muscle activity or mechanical interface pressures. To support RLI/RFI through multisensory stimulation, additional feedback channels besides the existing visual one can stimulate natural sensors of the human by artificial actuators in the orthosis. A promising candidate is haptic feedback, as it can stimulate the mechanoreceptors of the skin [23] and modify exteroception, i.e., tactile sensing, and proprioception including kinesthetic sensing of subject position, which are mostly perceived subconsciously and undergo very fast motor-reflective processing by the central nervous system [24]. Tactile feedback could be introduced by small vibrations on the skin, while kinesthetic feedback is implementable by inducing harmless mechanical resistances corresponding to the robot load at the human knee joint by an series elastic actuator. To optimize the effects of haptic feedback, the influence of the knees haptic paths on RLI should be examined and considered [12] by using the two point threshold method according to [12] for instance. Both types of feedback might enlarge the communication flow and potentially increase body schema integration and thus optimize control of the robot or prosthesis. Hence, tactile and kinesthetic feedback should be considered as independent variables as in Table I. In the experimental evaluation of user-feedback, it is important to create a consistent multisensory stimulation (see [10], [12]. Therefore, sensors and actuators

attached to the human should also be placed on the robot for example. Anyhow, from a design perspective it is an interesting issue to investigate illusion maintenance, if this is specifically ignored - e.g., if feedback is provided to the human but no corresponding actuator is visible at the robot. Hence, intended violations of consistency should be introduced as variables to derive rules for human-robot interfaces supporting body schema integration. Yet, it is worth noting that an operation without the orthosis is still required, as basic RFI/RLI experiments demand contactfree operation.

III. Robot Implementation

The practical implementation of the design prepared in [13] and the interface extensions is described subsequently.

A. Mechanics and Actuation

The implementation of the knee joint is depicted in the left part of Figure 2. It is driven by a DC gear motor 1.61.077.415 from Bühler Motor GmbH, Nürnberg, Germany with a gear ratio of $i_k = 1 : 135$ and a power of $4.34\,\mathrm{W}$. Connection to the knee shaft is realized by a bevel gear and a bellows coupling. The DC gear motor is overloaded to a peak power of about $10\,\mathrm{W}$ shortly, which is acceptable due to the manufacturer. The minimum knee angle φ_{min} of the implementation is $42\,^\circ$ and thus conflicts with the theoretical range of $30\,^\circ$ to $180\,^\circ$ required in [13]. As the measurements from real participants used there showed a minimum knee angle of $\varphi_{min} = 55\,^\circ$, the implementation is suited well, since practically requirements are not affected.

On the right side of Figure 2 the ankle joint realization that is driven by a DC motor 1.13.063.407 with $150\,\mathrm{W}$ supplied by Bühler Motor GmbH, Nürnberg, Germany via a timing belt is shown. This motor is loaded only partially and connected to a $1 : 40$ planetary gear and a timing belt with a transmission ratio of $4 : 5$. The resulting gear ratio of the ankle drive train is $i_a = 1 : 50$. The mechanical structure depicted left in Figure 3 provides the variation of shank and thigh lengths to suit different participants and comply with the requirements from [13]. The hull of shop-window mannequin and a nylon stocking are used to achieve a more natural outer appearance as shown in the middle part of Figure 3 and required in [13]. For more realistic outer appearance, a cosmetic cover for prostheses might be used. Customization to the user could be reached by dressing the robot with the same trousers as the subject.

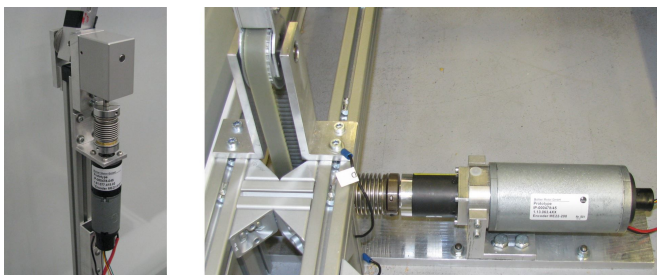

Fig. 2. Implementation of the knee (left) and ankle joint (right).

Fig. 3. Robot mechanics (left). Robot with cladding (middle). Interface orthosis (right, mirrored) with vibration motor positions (red circles).

B. Controls and Sensors

Controls and sensor data acquisition are implemented on a NI-9082 CompactRIO real-time control platform from National Instruments Germany GmbH, München, Germany. For the acquisition of human subject motion, a Microsoft Kinect RGB-D sensor is selected, while the positions and velocities of both robot joints are measured by incremental encoders on the drive shafts. Those have resolutions of $108,000$ and $40,000$ pulses per link revolution at knee and ankle.

C. Interface Extensions

In the right part of Figure 3 a first implementation of the knee interface orthosis using a Stabimed Pro soft orthesis from medi GmbH & Co. KG, Bayreuth, Germany is shown. Additional sensing of human data is provided by an incremental encoder measuring knee position and velocity. Those can be included in trajectory generation algorithms to improve results obtained using the RGB-D sensor only [21]. An intuitive haptic feedback might be reached by vibrations scaled proportionally to the mechanical knee load in amplitude or frequency. In design, sensitivity and processing of specific receptive fields should be considered: Small amplitudes and frequencies of $3 - 40\,\mathrm{Hz}$ stimulate Merkel's receptors and Meissner's corpuscles directly located below the epidermis of skin, while Pacinian corpuscles in the deeper dermal layer are sensitive to frequencies of $250 - 350\,\mathrm{Hz}$ [23]. A first implementation shown right in Figure 3 uses two vibration motors driven by a dual-channel DC driver board. The motors are positioned based on muscular activity during squats: Musculus rectus femoris and adductor magnus show high activity in electromyographic measurements [25] and are spatially accessible. VPM2 positions are given by red circles in Figure 3. Additional kinesthetic feedback will be introduced by applying resisting torques to the knee with a series elastic actuator and shared control concepts [26], [27].

IV. Modeling and Control

Based on the sketch given in Figure 1, the mechanical model of the Int^{2}Bot and the control algorithm are set up.

A. Modeling

The dynamic equations of the system are given by

$$\tau = M(q)\ddot{q} + C(\dot{q}, q) + G(q), \tag{1}$$

using Lagrange equations of the second kind [28]. The matrix $M(q) = [m_{11}\ m_{12}; m_{21}\ m_{22}]$ contains the elements given in Table II and matrices $C(\dot{q}, q)$ and $G(q)$ are specified as

$$C(\dot{q}, q) = \begin{bmatrix} -2\, l_s\, l_{t'}\, m_t\, \sin(\varphi)\, \dot{\varphi}^2 \ - l_s\, l_{t'}\, m_t\, \sin(\varphi)\, \dot{\psi}\, \dot{\varphi} \\ l_s\, l_{t'}\, m_t\, \sin(\varphi)\, \dot{\varphi}\, \dot{\psi} \end{bmatrix},$$

$$G(q) = \begin{bmatrix} g\ (l_{t'}\, m_t \sin(\psi + \varphi) + (l_{s'}\, m_s + l_s\, m_t)\ \sin(\psi)) \\ g\ (l_{t'}\, m_t\ \sin(\psi + \varphi)) \end{bmatrix}.$$

In the dynamic equations, $q = [\psi \quad \varphi]^T$ represents the vector of angular positions, $\tau = [\tau_a \quad \tau_k]^T$ is the torque vector. Considering that the Int^{2}Bot is adjustable to the leg length of the subject, the dynamics model can be adapted to different users by varying the lengths l_s and l_t of shank and thigh. Therefore, all parts of the shank with constant distance to the knee joint are referenced to the knee and transformed to the ankle joint considering the length of the shank of the participant. For the thigh, the mechanical parameters are referenced to the hip joint and transformed to the center of mass of the thigh considering the thigh length of the subject. The reduced inertia I_a of the shank with regard to the ankle joint including the ankle drive train is considered according to [29]. The inertia of the thigh with respect to its center of mass is represented by I_t and the inertia of the rotor in the knee drive is given by I_{rt}. The model parameters given in Table III are determined from the CAD model and by weighing the parts to match the real system.

TABLE II

ELEMENTS OF THE MASS MATRIX

Elem.	**Content**
m_{11}	$I_a + 2\, I_t + m_t\, \left(l_s^2 + 2\, \cos(\varphi)\, l_s\, l_{t'} + l_{t'}^2\right)$
$m_{12} = m_{21}$	$2\, I_t + m_t\, \left(l_{t'}^2 + \ l_s\, \cos(\varphi) l_{t'}\right)$
m_{22}	$m_t\, l_{t'}^2\, I_{rt} + 2\, I_t$

TABLE III

PARAMETERS OF MECHANICAL SETUP AND CONTROL

	Parameter	**Value**	**Unit**	**Description**
mechanics	I_a	16.939	kgm^2	reduced ankle inertia
	I_{rt}	0.0305	kgm^2	knee actuator inertia
	I_t	0.0062	kgm^2	thigh interia
	m_s	0.8001	kg	shank mass
	m_t	0.2054	kg	thigh mass
	l_s	0.6	m	shank length
	l_t	0.6	m	thigh length
	$l_{s'}$	0.4557	m	dist. COM(shank)-ankle
	$l_{t'}$	0.3411	m	dist. COM(thigh)-knee
	g	9.81	$\frac{m}{s^2}$	gravity
control	$k_{p,a}$	169	$Nm\ rad^{-1}$	proportional gain, ankle
	$k_{v,a}$	26	$Nm\ s\ rad^{-1}$	derivative gain, ankle
	$k_{p,k}$	169	$Nm\ rad^{-1}$	proportional gain, knee
	$k_{v,k}$	26	$Nm\ s\ rad^{-1}$	derivative gain, knee

B. Control

For motion control, a computed torque algorithm linearizing the closed-loop system by compensating inertia and gravity effects [28] is combined with a fuzzy-based friction compensation. The controller is realized based on the analytical inverse dynamics model (1) and a PD feedback controller. The control law is

$$\begin{aligned} \tau &= M(q)\ \left[\ddot{q}_d + k_p\, \tilde{q} + k_v\, \dot{\tilde{q}}\right] + C(\dot{q}, q) + G(q) + \tau_{FC} \\ &= \tau_m + C(\dot{q}, q) + G(q) + \tau_{FC}\,, \end{aligned} \tag{2}$$

where the matrices $M(q)$, $C(\dot{q}, q)$ and $G(q)$ are the ones given in (1) and τ_{FC} represents the torque of friction compensation. Further, the diagonal matrices $k_p = diag(k_{p,a} \quad k_{p,k})$ as well as $k_v = diag(k_{v,a} \quad k_{v,k})$ contain the control parameters and the vector $\tilde{q} = q_d - q$ represents the control error. Assuming that the dynamics model matches the real robot and friction is compensated ideally, the linearized closed-loop behavior is given by

$$\ddot{\tilde{q}} + k_v\, \dot{\tilde{q}} + k_p\, \tilde{q} = 0\,. \tag{3}$$

To adjust closed-loop dynamics to yield critical damping, control parameters are chosen to be $k_p = \omega^2$ and $k_v = 2\,\omega$, where ω is the exponential decay rate of the errors $\tilde{q}$ and $\dot{\tilde{q}}$ [28]. Corresponding numeric values resulting in fast reactions without overshooting are given in Table III.

C. Friction Compensation

Experiments have shown that the joint mechanics inherit coulomb and vicious friction that can be modeled as

$$\tau_F = \tau_C\, sign(\dot{q}) + a_V\, \dot{q}, \tag{4}$$

for $\dot{q} \neq 0$, while stiction effects occur, if $\dot{q} = 0$ [30]. In this, τ_F is the friction torque. The diagonal matrices $\tau_C = diag(4.02\,\mathrm{N\,cm} \quad 0.16\,\mathrm{N\,cm})$ and $a_V = diag(0.45\,\mathrm{N\,mm\,rpm^{-1}} \quad 0.016\,\mathrm{N\,mm\,rpm^{-1}})$ contain the coefficients of Coulomb and viscous friction of ankle and knee. As computed torque control only takes into account the gravitational, coriolis and inertial effects [28], the friction compensation algorithm from [31] is implemented based on (4) as shown in Figure 4. It uses a fuzzy-membership function for a weighted superposition of two friction compensation torques depending on joint velocities. The compensation torques are determined based on τ_m and do not

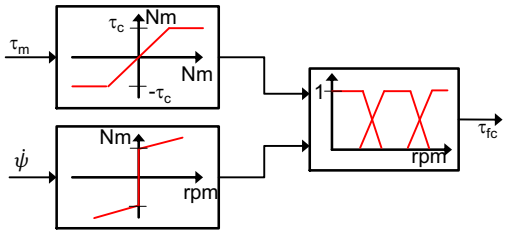

Fig. 4. Friction Compensation

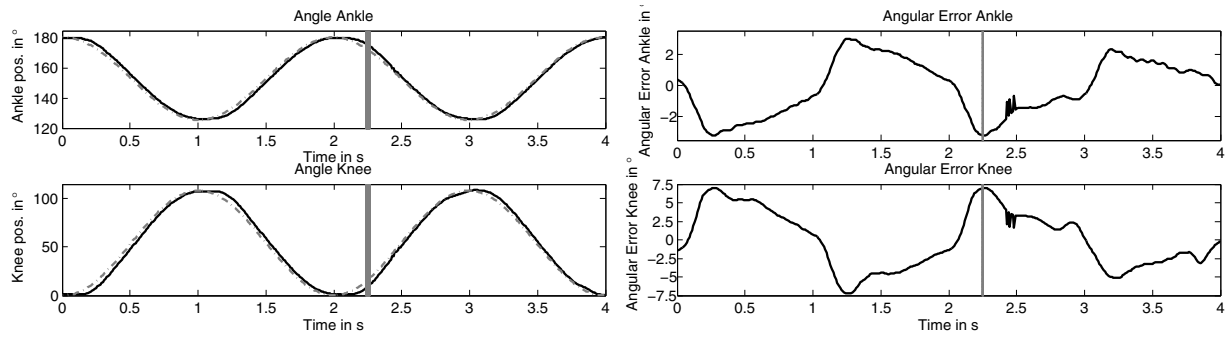

Fig. 5. Squats at 0.5 Hz. Friction compensated after 2.25 s (grey line). Left - Position/reference (solid black/dash-dotted grey). Right - Control error.

include stiction. For low velocities, only Coulomb friction is compensated by selecting torques from the characteristic curves that are smoothened by ramps to avoid fast switching due to sensor noise. For high velocities, friction compensation torques are determined based on the complete characteristics and using the specific joint velocity. With this, friction can be compensated before the joint moves and the influence of sensor noise is reduced. The torque parameters of friction compensation are selected to be lower than the real friction parameters to avoid overcompensation. Further parameters of the ramp smoothing the compensation of Coulomb friction and the fuzzy-membership functions are obtained heuristically in experiments.

V. Experiments

To investigate the dynamical operation and control of the Int^{2}Bot, its tracking performance is examined experimentally. As discussed in [13], the duration of a fast human squat is about 2 s and thus squat frequencies of up to 1 Hz are investigated to consider extreme situations. To evaluate control performance, synthetic trajectories close to human squats are used, while experiments with a human subject were performed to examine the performance of the overall setup and to analyze the occuring delays.

A. Synthetic trajectories

Synthetic sinusoidal trajectories, which are comparable to biomechanical ones, are used as desired trajectories for evaluation. Position amplitudes are $0\,^\circ$ to $110\,^\circ$ for the knee angle φ and $125\,^\circ$ to $180\,^\circ$ for the ankle angle ψ. In the left part of Figure 5, the angular motions of ankle and knee are shown at a squat frequency of 0.5 Hz. Starting with computed torque control only, the friction compensation is activated at 2.25 s (vertical grey line). The desired trajectory is presented in grey and the measured one is given in black. Although a slight phase shift occurs between desired and real trajectories due to unmodeled dynamics and friction, good overall tracking performance can be observed.

The influence of friction compensation becomes distinct by comparing positions and errors before and after its activation in Figure 5. The mean errors of ankle and knee positions reduce from $e_\psi = 1.79\,^\circ$ and $e_\varphi = 3.91\,^\circ$ to $e_\psi = 1.27\,^\circ$ and $e_\varphi = 2.84\,^\circ$. This means that the proposed friction compensation reduces the mean position error by up to 50%. Due to the structural change in the controller at 2.25 s, small disturbances appear and decay at about 2.5 s. As this change in the controller is only performed for analysis, such disturbances will not appear or affect operation.

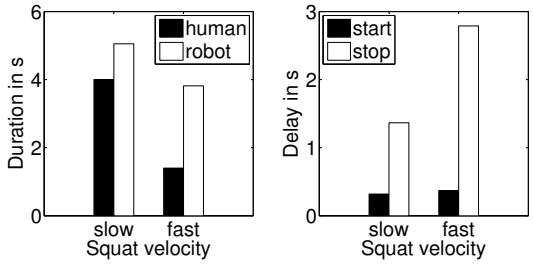

Fig. 6. Bar plots of motion duration (left) and motion delay (right).

B. Human trajectories

A first investigation of the delays between human motions and robot imitation are evaluated using a Casio Exilim FH-20 camera at 1000 fps in [32]. Durations of human and robot movement and their delays are compared in Figure 6 based on data acquired in this study for slow and fast motions, where velocities were selected by the subject. While human motions show durations of 4.00 s for the slow and 1.40 s for the fast codition, those of the robot are significantly slower with 5.05 s and 3.82 s respectively. Accordingly, the delay in starting the motion is distinctly smaller than in stopping it with 0.32 s and 1.37 s in slow squats as well as 0.37 s and 2.79 s in fast squats. As these significant delays between human and robot motion exceed the requirements from [13], only preliminary body schema integration experiments can be performed so far. To reduce the delays, measurements of the knee orthosis can be fused with RGB-D data or improved motion tracking can be introduced, as the delays result from high estimation errors in skeleton tracking [21].

VI. Conclusions

This paper deals with the implementation, practical control and user-feedback of the Int^{2}Bot. By mimicking human motions during a squat task, it is designed to investigate the

integration of artificial devices into the body schemas of their users in terms of a Rubber Leg Illusion. To investigate the impact of novel interface technologies, the psychological test design is extended compared to the one from [13] to comprise haptic and kinesthetic user-feedback. The mechatronic implementation is therefore complemented by an actuated and instrumented knee orthosis in Section II. For the control of the robot, computed torque control is combined with a fuzzy-based friction compensation as shown in Section IV. Experiments without a user given in Section V show good tracking results and a reduction of position errors by up to 50% through the friction compensation. Although limited by knee actuation, the robot can perform considerably fast squats with $0.8\,\mathrm{Hz}$, which comes up to maximum human capabilities. Evaluating the robot with a human user shows that the setup is currently limited by trajectory generation due to delays caused by errors in RGB-D skeleton tracking and the related data transfers [21]. Hence, only preliminary body schema integration experiments can be performed.

Future works aim at reducing delays with additional or improved motion sensing to improve psychological experiments. Those will be deducted including investigations of user-feedback and multisensor-integration [23]. Additionally, the authors consider implementing harmless and quasi-static temperature-feedback [24] to encode device state or fault warnings as adaptive-temperature-nociceptive information - e.g., a colder interface in case of low battery.

ACKNOWLEDGMENT

The authors thank Bühler Motor GmbH, medi GmbH & Co. KG and National Instruments Germany for donations.

REFERENCES

[1] H. Senra, R. Aragao Oliveira, I. Leal, and C. Vieira, "Beyond the body image: a qualitative study on how adults experience lower limb amputation," *Clinical Rehabilitation*, vol. 26, pp. 180 – 191, 2011.

[2] A. Mayer, K. Kudar, K. Bretz, and J. Tihanyi, "Body schema and body awareness of amputees," *Prosthetics and Orthotics International*, vol. 32(3), pp. 363–82, 2008.

[3] S. Gallagher and J. Cole, "Body Schema and Body Image in a Deafferented Subject," *Journal of Mind and Behavior*, vol. 16, pp. 369–390, 1995.

[4] O. Horgan and M. MacLachlan, "Psychosocial adjustment to lower-limb amputation: A review," *Disability and Rehabilitation*, vol. 26, pp. 837–850, 2004.

[5] C. Murray and J. Fox, "Body image and prosthesis satisfaction in the lower limb amputee," *Disability and rehabilitation*, vol. 24 (17), pp. 925–931, 2002.

[6] A. I. Goller, K. Richards, S. Novak, and J. Ward, "Mirror-touch Synaesthesia in the Phantom Limbs of Amputees," *Cortex*, vol. http://dx.doi.org/10.1016/j.cortex.2011.05.002, 2012.

[7] M. Botvinick and J. Cohen, "Rubber hands 'feel' touch that eyes see," *Nature*, vol. 391, p. 756, 1998.

[8] O. Christ, M. Jokisch, J. Preller, P. Beckerle, S. Rinderknecht, and J. Vogt, "Persistence of the rubber hand illusion and maintaining factors during active or passive movements: new indicators for rehabilitation?" *European Psychiatry*, vol. 27 (S1), p. 224, 2012.

[9] O. Christ and M. Reiner, "Perspectives and possible applications of the rubber hand and virtual hand illusion in non-invasive rehabilitation: Technological improvements and their consequences (in press)," *Neuroscience and Biobehavioral Reviews*, 2014.

[10] B. Rosen, H. H. Ehrsson, C. Antfolk, C. Cipriani, F. Sebelius, and G. Lundborg, "Referral of sensation to an advanced humanoid robotic hand prosthesis," *Scandinavian Journal of Plastic and Reconstructive Surgery and Hand Surgery*, vol. 43, pp. 260–266, 2009.

[11] M. Jokisch, J. Preller, A. Schropp, O. Christ, P. Beckerle, and J. Vogt, "The rubber hand illusion paradigm transferred to the lower limb: A physiological, behavioral and psychometric approach," *International Journal of Psychophysiology*, vol. 85 (3), pp. 421–422, 2012.

[12] O. Christ, A. Elger, K. Schneider, P. Beckerle, J. Vogt, and S. Rinderknecht, "Identification of haptic paths with different resolution and their effect on body scheme illusion in lower limbs," *Technically Assisted Rehabilitation*, 2013.

[13] P. Beckerle, O. Christ, J. Wojtusch, J. Schuy, K. Wolff, S. Rinderknecht, J. Vogt, and O. von Stryk, "Design and control of a robot for the assessment of psychological factors in prosthetic development," *IEEE International Conference on Systems, Man, and Cybernetics*, 2012.

[14] P. Beckerle, O. Christ, M. Windrich, G. Schütz, J. Vogt, and S. Rinderknecht, "User-centered prosthetic design: A methodological approach to transfer psychological factors to technical development," *Technically Assisted Rehabilitation*, 2013.

[15] O. Christ, P. Beckerle, S. Rinderknecht, and J. Vogt, "Usability, satisfaction and appearance while using lower limb prostheses: Implications for the future," *Neuroscience Letters*, vol. 500 (S1), p. e50, 2011.

[16] E. Lewis and D. M. Lloyd, "Embodied experience: A first-person investigation of the rubber hand illusion," *Phenomenology and the Cognitive Sciences*, vol. 9, pp. 317–339, 2010.

[17] M. R. Longo and P. Haggard, "Sense of agency primes manual motor responses," *Perception*, vol. 38, pp. 69–78, 2009.

[18] K. C. Armel and V. S. Ramachandran, "Projecting sensations to external objects: evidence from skin conductance response," *Proceedings of the Royal Society, B, Biological Sciences*, vol. 270, pp. 1499–1506, 2003.

[19] M. Slater, D. Perez-Marcos, H. H. Ehrsson, and M. V. Sanchez-Vives, "Inducing illusory ownership of a virtual body," *Frontiers in Neuroscience*, vol. 3 (2), pp. 214–220, 2009.

[20] M. P. M. Kammers, K. Rose, and P. Haggard, "Feeling numb: Temperature, but not thermal pain, modulates feeling of body ownership," *Neuropsychologia*, vol. 49, pp. 1316–1321, 2011.

[21] F. Schültje, P. Beckerle, M. Grimmer, J. Wojtusch, and S. Rinderknecht, "Comparison of Trajectory Generation Methods for a Human-Robot Interface based on Motion Tracking in the Int^{2}Bot," *IEEE International Symposium on Robot and Human Interactive Communication*, 2014.

[22] F. Amigoni, V. Schiaffonati, and M. Somalvico, "A theoretical approach to human-robot interaction based on the bipolar man framework," *IEEE International Workshop on Robots and Human Interactive Communication*, 2002.

[23] E. Burdet, F. D. W, and T. E. Milner, *Human Robotics - Neuromechanics and Motor Control*. MIT Press, 2013.

[24] D. Zühlke, *Nutzergerechte Entwicklung von Mensch-Maschine-Systemen: Useware-Engineering für technische Systeme*. Springer, 2012.

[25] F.-C. Kuo, W.-P. Kao, H.-I. Chen, and C.-Z. Hong, "Squat-to-reach task in older and young adults: Kinematic and electromyographic analyses," *Gait & Posture*, vol. 33, pp. 124–129, 2011.

[26] Y. Yokokohji and T. Yoshikawa, "Bilateral control of master-slave manipulators for ideal kinest het ic coupling," *IEEE International Conference on Robotics and Automation*, 1992.

[27] H. Boessenkool, A. D. Abbink, C. J. M. Heemskerk, F. C. T. van der Helm, and J. G. W. Wildenbeest, "A task-specific analysis of the benefit of haptic shared control during telemanipulation," *IEEE Transactions on Haptics*, vol. 6 - 1, pp. 2 – 12, 2013.

[28] R. Kelly, V. Santibáñez Davila, and J. A. Loría Perez, *Control of Robot Manipulators in Joint Space*. Springer, 2005.

[29] D. Gross, W. Hauger, J. Schröder, and W. A. Wall, *Technische Mechanik 3: Kinetik*. Springer, 2010.

[30] B. Bona and M. Indri, "Friction compensation in robotics: an overview," *44th IEEE Conference on Decision and Control, and the European Control Conference*, 2005.

[31] S. Rinderknecht and B. Strah, "Simple and effective friction compensation on wheeled inverted pendulum systems," *Euro-Mediterranean Conference on Structural Dynamics and Vibroacoustics*, 2013.

[32] O. Christ, J. Wojtusch, and P. Beckerle, "Robotic mirroring of movements in the lower limbs: signal delay of a consumer device sensor," *SAN2014 Meeting Book of Abstracts*, 2014.